Effect of Coupled Synchro-Betatron Oscillation on the Stability of Single Particle Motion in ELETTRA

R. Nagaoka and L.Tosi
Sincrotrone Trieste, Padriciano 99, 34012 Trieste, Italy

Abstract

A 6-dimensional symplectic transformation scheme is developed in the tracking code RACETRACK, also incorporating 6-dimensional integrators through the field of insertion devices. Application is made to ELETTRA in the presence of both insertion device and magnet imperfections.

1. INTRODUCTION

Tracking studies are of great importance in a dedicated low-emittance machine such as ELETTRA. This is because of a large reduction in the transverse stability generally due to sextupoles, magnet errors, and nonlinear fields of insertion devices. Usually therefore, one is most interested in tracking the transverse coordinates under a fixed energy. However, since in reality a particle is oscillating both transversely and longitudinally, the former investigations may not be adequate if there is a significant coupled effect between different modes.

In ELETTRA, the low-emittance optics results in a small frequency for the energy oscillation upon which it was found [1] that satellite synchro-β resonances would not be serious since resonance conditions are far from being fulfilled. Nevertheless, a synchrotron oscillation period amounts to only as many as 100 revolutions so that a possible modulation of the transverse motion occuring in this interval due to the coupling may be suspected to influence the stability, as it has been found by the ALS group to be the case in the analysis of their machine [2].

To examine the effect, a fully 6-dimensional symplectic transformation routine has been developed in RACETRACK [3] considering the path length effect up to second order in the transverse angles [4]. Together with this, the symplectic integration routines for insertion devices in RACETRACK [5,6] are extended to incorporate the longitudinal degree of freedom. The obtained tool is applied to ELETTRA taking both insertion device and magnet imperfections into account.

2. DESCRIPTION OF THE NUMERICAL APPROACH

Among a number of works already existing on the unified description of transverse and longitudinal motion, here that developed by the DESY group [7] has been followed. The Hamiltonian for a relativistic electron may be given by

$$H = -\kappa x\,(1+\delta) - (1+\kappa x)\frac{e}{E_0}A_s + \frac{1}{2}\frac{\left[\,(p_x - \frac{e}{E_0}A_x)^2 + (p_y - \frac{e}{E_0}A_y)^2\,\right]}{(1+\delta)} \qquad (1)$$

where $\mathbf{A} = (A_x, A_y, A_s)$ is the vector potential with components defined in the frame (x, y, s), where s measures the arc length of the reference orbit at nominal energy E_0, and x and y are the transverse coordinates. The reference orbit is assumed to lie on the horizontal plane whose curvature is denoted by κ. The canonical variables are $(x, p_x, y, p_y; \sigma, \delta)$ in which $\sigma = s - ct$ (c: light velocity, t: time) measures the longitudinal position with respect to the reference particle and $\delta = (p - p_0)/p_0$ describes the momentum deviation.

All electromagnetic fields in the ring apart from insertion devices are expressed with appropriate forms of A_s (i.e. $A_x = A_y = 0$). Since in an electron storage ring, r.f. cavities are accelerating to compensate the radiation energy loss, the mean energy loss is subtracted from the energy gain in a cavity to simplify the model. The variable δ being constant in the rest of the ring, conventional transfer matrices are used to transform (x, x', y, y') over the linear elements. Nonlinear elements such as sextupoles are treated as usual as pointlike. From Eq. 1 it follows that

$$\sigma(s) = \sigma(s_0) - \int_{s_0}^{s} \left[\kappa x + \frac{1}{2}(x'^2 + y'^2)\right] ds. \qquad (2)$$

Namely, the variation of path length of a trajectory is considered up to second order in transverse angles, which can be solved analytically for all linear elements [7]. More details on the above descriptions are found in Refs. 4 and 7.

The fields of insertion devices are treated by the analytical expressions which may be derived by the appropriate form of A_x and A_y (i.e. $A_s = 0$). Having both linear and nonlinear fields over a finite length, one needs to integrate the motion explicitly through the device. So far two different symplectic schemes have been implemented into RACETRACK: (i) The application of the canonical integration technique [8] in second order, thus guaranteeing the accuracy up to 2nd order in the time increment [5]. (ii) The symplectic wiggler transformation recently proposed by Bahrdt and Wüstefeld [9,10]. While the basis of the former is the "leap frog method" with which the required number of steps per period of the field can be reduced, the latter derives a Taylor-expanded generating function [10] which may allow a transformation over a step even larger than a period length, thus manifesting a great superiority. With some extensions made in the latter approach in the second-order formulation [6], both routines implemented in RACETRACK are capable of treating the general nonplanar devices with an arbitrary step size.

In course of the present study, both schemes have been extended to include the longitudinal degree of freedom, namely to include variables σ and δ, on the basis of the Hamiltonian

in Eq. 1. Details will be found in Ref. 11. The six-dimensional tracking scheme as well as the extended integration routines for insertion devices will be incorporated in the new version of RACETRACK to appear [12].

3. NUMERICAL RESULTS

The method presented previously is applied to ELETTRA at 1.5 GeV, whose major related parameters are summarized in Table 1. The ring consists of 12 Chasman Green cells, in which the dispersive section between two dipoles are expanded to optimize the low-emittance optics. Cavities are placed in these expanded free straight sections. All dynamic aperture calculations have been made by tracking a particle over 1000 turns which corresponds nearly to 10 synchrotron periods.

Table 1. Related parameters of ELETTRA.

Circumference [m]	259.2
Linear Tunes $Q_x/Q_y/Q_s$	14.305/8.201/0.011
Natural Emittance $\varepsilon_{x\beta}$ [m·rad]	3.93×10^{-9}
Momentum Compaction α_c	1.58×10^{-3}
Number of Cavities	4
R.F. Frequency [MHz]	499.654
Peak Effective Voltage [MV]	1.7
Total Radiation Loss [KeV/turn]	128
Synchronous Phase [deg]	4.318
RF bucket Size $\Delta E/E_0$	0.0305
Relative Energy Spread σ_E ($\Delta E/E_0$)	0.0006
Damping Times $\tau_x/\tau_y/\tau_\varepsilon$ [msec]	24.2/31.9/18.9

Investigations of the dynamic apertures have been first carried out in the ideal machine without errors in the presence of a wiggler with maximum on axis field B_0 = 1.15 T and period length λ_0 = 14 cm.

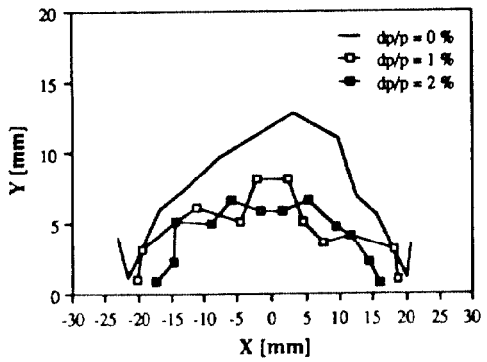

Figure 1. Dynamic apertures with a wiggler in the absence of errors.

Figure 1 shows the dynamic apertures of the motion oscillating in energy with different initial deviations. It must be mentioned that there is a significant reduction in both the horizontal and the vertical maximum stable amplitudes with respect to the corresponding cases without the device, which are not shown. However, by comparing numerically the results in Fig. 1 with the dynamic apertures obtained with the same non-oscillating energy deviations, a reduction of about 2 mm in the maximum vertical stable amplitudes in the oscillating case is observed, whereas no effective difference occurred in the horizontal ones.

Simulations have been also accomplished in the ideal lattice with a realistic scenario of insertion devices, in which in addition to the above wiggler, five undulators with fields varying between 0.46 T and 0.63 T and period lengths in the range between 5.6 cm and 12.5 cm were introduced.

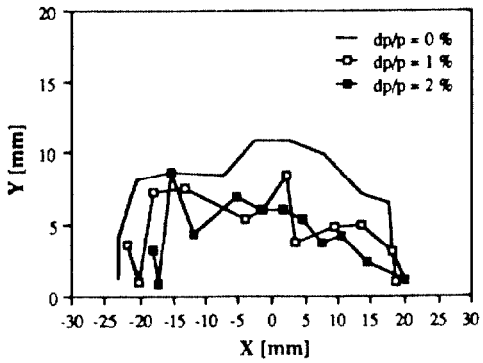

Figure 2. Dynamic apertures of the ideal lattice with a realistic scenario of insertion devices.

The resulting dynamic apertures including the energy oscillations with different initial deviations are reported in Fig. 2. Also in this case, it has been found that the oscillation in energy with respect to the constant energy deviation case leads to no significant further reduction.

Since similar behaviour has been observed also for an undulator (B_0 = 0.63 T and λ_0 = 7.3 cm), it may be concluded that the main source of the reduction with respect to the bare lattice comes from the presence of the devices and the additional degree of freedom introduced by the longitudinal motion combined with the devices does not bring a further drastic reduction.

We now consider the case of including the previous wiggler in the ring in the presence of errors. The assumed errors are the Gaussian distributed random errors of alignment, rotation and field strength, considered for dipoles, quadrupoles and sextupoles. The rms values employed are listed in Table 2. Ten machines each differing in the error distribution have been generated in which the closed orbit distortions (COD) are corrected with monitors and correctors, using the routines provided by RACETRACK, leaving the residual COD at monitor positions to be in the range of a few tenths of a milimeter.

Table 2. RMS values of magnet errors assumed.

	Dipole	Quadrupole	Sextupole
Field error	0.12%	0.1%	0.1%
Misalignment		0.2 mm	0.2 mm
Tilt	0.5 mrad	0.2 mrad	0.2 mrad

The dynamic apertures of a particle oscillating in energy with 2% deviation are shown in Fig. 3. For comparison, those of

the non oscillating case at $\delta = 0$ are also plotted. These results are obtained with the betatron tunes refitted to the ideal values prior to the tracking. The reduction in the aperture of 5 ~7 mm is observed in both transverse directions compared to $\delta = 0$ case. A similar reduction with synchrotron oscillation has been observed also in the absence of the insertion device [4].

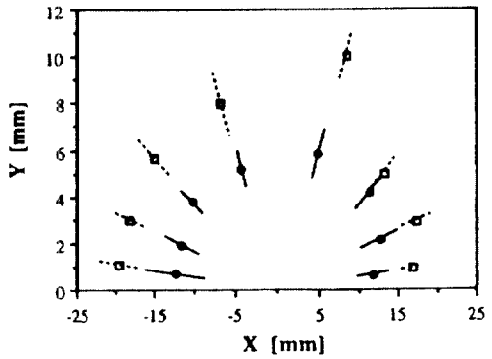

Figure 3. Dynamic apertures with a wiggler in the presence of errors. Symbols and bars represent averages and rms over 10 machines, respectively. Circles: 2% oscillation. Squares: Energy fixed at nominal value.

The computation without tune fitting has also been done resulting in nearly identical average dynamic apertures, but in larger rms deviations implying the high sensitivity of the stability to transverse tunes.

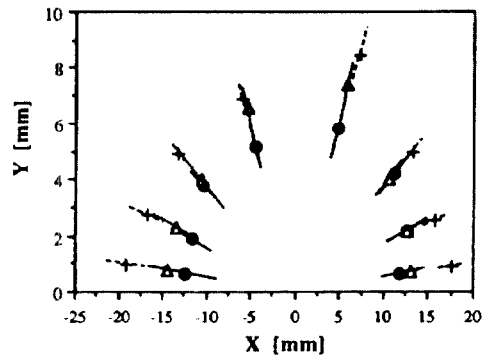

Figure 4. Comparison of dynamic apertures between oscillatory and non-oscillatory motions in energy. Circles: 2% oscillation. Triangles: +2% fixed. Crosses: -2% fixed.

To see the effect of longitudinal oscillation on the dynamic aperture in more detail, those of the oscillating case at 2% are displayed in Fig. 4 together with apertures of fixed off-energy motion at ±2%, respectively. The results shown are obtained without tune fitting. One finds that, although the dynamic aperture is, on the whole, further reduced with the oscillation, the reduction with respect to the minimum of the two fixed off energy cases are of a few milimeters and small compared to the reduction found in Fig. 4, which is in accordance with the feature observed in other cases.

4. CONCLUSION

To investigate the stability of a single particle motion performing the coupled synchro-β oscillation, a 6-dimensional symplectic tracking algorithm has been introduced in RACETRACK on the basis of the work of Ref. 7. Together with this, the symplectic integration routines through the field of insertion devices have been extended to include the additional longitudinal degree of freedom.

The obtained tool has been applied to ELETTRA at 1.5 GeV to evaluate the dynamic apertures in the presence of insertion devices and possible magnet errors. The main feature observed may be the aperture reduction with the synchrotron oscillation included, as compared to those at fixed nominal energy. However, the coupled longitudinal oscillation itself did not seem to be the main cause for the observed reduction, as has been found from the comparison to those of the corresponding fixed off-energy motions. To have a deeper understanding of the effect of coupled oscillation on the characteristics of the motion would however require some further analysis.

5. ACKNOWLEDGEMENT

The authors thank Dr. A. Wrulich for the suggestion of this work as well as for helpful discussions, and Dr. R.P. Walker for providing them with the parameters of the insertion devices.

6. REFERENCES

[1] L. Tosi and A. Wrulich, "Satellite Resonances generated by Cavities in the Dispersive Region of the Arc", ST/M-87/14.

[2] E. Forest, R. Keller, H. Nishimura and M.S. Zisman, "Study of a Relaxed ALS Storage Ring Lattice", LSAP-076, ESG Note-82 (1989); A. Jackson, private communication (1989).

[3] A. Wrulich, "RACETRACK", DESY Report 84-026 (1984); F. Iazzourene et al., "RACETRACK User's Guide, Version 4.00", ST/M-91/11.

[4] R. Nagaoka, "Effect of Coupled Synchro-Betatron Oscillation in the ELETTRA Storage Ring", ST/M-91/20.

[5] R. Nagaoka and L. Tosi, "An Improved Scheme for Integrating the Particle Motion through the Insertion Device in RACETRACK", ST/M-90/6.

[6] R. Nagaoka and L. Tosi, "An Extended Scheme of the New Tracking Routine for Nonplanar Insertion Devices", ST/M-91/4.

[7] D.P. Barber, G. Ripken and F. Schmidt, "A Nonlinear Canonical Formalism for the Coupled Synchro-Betatron Motion of Protons with Arbitrary Energy", DESY Report 87-036.

[8] R.D. Ruth, "A Canonical Integration Technique", AIP Conf. Proc. **153** (1987) pp. 150.

[9] J. Bahrdt and G. Wüstefeld, "A New Tracking Routine for Particles in Undulator and Wiggler Fields: Part I and II", BESSY TB Nr. 158, October 1990; J. Bahrdt, "A New Tracking Routine for Particles in Undulator and Wiggler Fields: Part III", BESSY TB Nr. 158, October 1990.

[10] J. Bahrdt and G. Wüstefeld, "A Taylor-Expanded Generating Function for Particle Motion in Arbitrary Magnetic Fields", in this conference.

[11] R. Nagaoka and L. Tosi, to appear as an internal report.

[12] F. Iazzourene et al., in progress.